Environmental Science
Processes & Impacts

Influence of microorganisms on uranium release from mining-impacted lake sediments under various oxygenation conditions

Journal:	*Environmental Science: Processes & Impacts*
Manuscript ID	EM-ART-03-2022-000104.R2
Article Type:	Paper

Environmental significance statement

After their closure, uranium (U) mine wastes constitute a potential source of radionuclides to surface environments, which need to be appropriately monitored and managed through time. Lake and pond sediments that have been significantly enriched in U because of former U mining activities can be allowed to be dredged and stored in a surface storage site. Little is known regarding the potential effect of these treatments on uranium mobilization, especially if these sediments were anoxic prior to dredging operations. Midly oxygenated conditions yielded the lowest U release rate even if U(IV) solid species in the sediments were fully oxidized. This result is interpreted as U(VI) scavenging mechanism by iron-oxyhydroxides produced from microbial Fe(II) oxidation.

Influence of microorganisms on uranium release from mining-impacted lake sediments under various oxygenation conditions

Marina Seder-Colomina[a], Arnaud Mangeret[a,*], Pascale Bauda[b], Jessica Brest[c], Lucie Stetten[a,c], Pauline Merrot[c], Anthony Julien[a], Olivier Diez[a], Evelyne Barker[a], , Elise Billoir[b], Pascal Poupin[b], Antoine Thouvenot[d], Charlotte Cazala[a], Guillaume Morin[c]

[a]Institut de Radioprotection et de Sûreté Nucléaire (IRSN), PSE-ENV/SEDRE, 31 avenue de la Division Leclerc, 92260 Fontenay-aux-Roses, France.

[b]Université de Lorraine, CNRS, LIEC, F-57000 Metz, France

[c]Institut de Minéralogie, de Physique des Matériaux et de Cosmochimie (IMPMC), UMR 7590 CNRS-Sorbonne Université -MNHN-IRD, case 115, 4 place Jussieu, 75252 Paris Cedex 5, France

[d]Athos Environnement, 63171 Aubière, France

To be submitted to Environmental Science: Processes & Impacts

*Corresponding author: arnaud.mangeret@irsn.fr

Tel +33 1 58 35 76 95

Fax +33 1 46 57 62 58

ABSTRACT

Microbial processes can be involved in the remobilization of uranium (U) from reduced sediments under O_2 reoxidation events such as water table fluctuations. Such reactions could be typically encountered after U-bearing sediment dredging operations. Solid U(IV) species may thus reoxidize into U(VI) that can be released in pore waters in the form of aqueous complexes with organic and inorganic ligands. Non-uraninite U(IV) species may be especially sensitive to reoxidation and remobilization processes. Nevertheless, little is known regarding the role of microbially mediated processes on the behaviour of U under these conditions.

In this study, laboratory incubation experiments were performed, under three different oxygenation conditions (0, 50 and 100% O_2-saturation, referred to as oxic, hypoxic and anoxic). The incubation experiments were conducted on fresh sediments from Lake Saint-Clement formely impacted by U mining activities, and containing ~300 mg/kg of U, mainly under the form of mononuclear U(IV) species (60-80%). XANES analysis of the incubated sediments shows that U(IV) was fully oxidized to U(VI) under oxic and hypoxic conditions and remained U(IV) under anoxic conditions. Nevertheless, hypoxic conditions lead to the lowest U release in solution after three weeks (3.6 $\mu g.L^{-1}$), whereas oxic and anoxic conditions slightly favored U release (8.3 – 15.5 $\mu g.L^{-1}$, respectively). Geochemical modeling suggested that U was mainly released as aqueous U(VI)-carbonate and Ca-U(VI)-carbonate complexes under oxic/hypoxic and anoxic conditions, respectively. Semi-confined hypoxic conditions were found to stimulate microbial Fe^{2+} oxidation, which lowers the pH, limits U complexation to bicarbonate ions and potentially produces ferric-oxyhydroxides able to sorb U(VI). Molecular analyses yield genomic evidence for an increasing abundance of Fe oxidizers under these conditions and thus support their possible role in decreasing U mobility.

1. INTRODUCTION

Uranium (U) is one of the most common and persistent subsurface contaminants from the front end of the nuclear cycle, such as former U mining activities; notably due to its long half-life of 4.4 billion years and its chemical and radiological toxicities to human beings and biota [1]. In France, the extraction of U by open-pit and underground mining has concerned approximately 250 sites, from 1948 to 2001 [2]. After their closure, U mine wastes, including mill tailings, waste rocks and mining-impacted soils and sediments, constitute a potential source of radionuclides to surface environments, which need to be appropriately monitored and managed through time. Several studies have shown that U can accumulate in reducing environments such as wetlands [3-7], alluvial aquifers [8] and lake sediments [9-10] downstream from U mining and processing sites. In France, lake and pond sediments that have been significantly enriched in U because of former U mining activities can be allowed to be dredged and stored in a surface storage site. Depending on the physico-chemical conditions these operations could potentially induce transformations of the U redox state and mobility in sediments [11]. Moreover, little is known regarding the potential effect of these treatments on microbial activities, especially if these sediments were anoxic prior to dredging operations.

The long-term efficiency of U retention in sediments is largely controlled by the nature of the U chemical species [12-13], pH and redox regimes [14]. The presence of organic [15-16] and inorganic carbon [11,17] as well as other inorganic ligands [18] is also an important factor to consider. Notably U(VI) is known to form highly mobile stable complexes with carbonates such as $UO_2(CO_3)_2^{2-}$, conversely to sparingly soluble U(IV) species [19]. In addition, biological activity can directly or indirectly modify U speciation and significantly lower U mobility[19]. For instance, enzymatic microbial reduction of U(VI) can directly lead to the formation of low-soluble U(IV) species [21-22]. Moreover, indirect reduction of U(VI) to U(IV) can be favoured by

Fe(II)-rich phases such as bio-reduced phyllosilicates [10,23] or green rusts [24]. On the contrary it has been shown that under slightly acidic laboratory conditions Fe(III)-bearing minerals may reoxidize bio-uranitite or biogenic U(IV) with a release of dissolved Fe(II) [25-26]. Microbial alkaline phosphatase activity may also induce periplasmic precipitation of U(VI)-phosphate minerals[27]. Finally, biosorption to bacterial surfaces and exopolymers [28-30] as well as to mineralized cells and biofilms [30-33] are also important U scavenging mechanisms.

Lake Saint-Clément, situated in the Massif-Central (France) is an artificial reservoir impacted by discharges of treated U mine waters from the site of Bois-Noirs Limouzat [9]. Detailed geochemical and mineralogical analyses of well-preserved sediment cores from this Lake [9-10] suggested that early diagenesis processes below the sediment-water interface lead to the indirect reduction of U(VI) to mononuclear U(IV) species by Fe(II) produced from the bioreduction of Fe(III)-rich chlorite, e. g. chamosite. In the same studies, X-ray absorption spectroscopy of the samples indicated that these early-diagenetic U(IV) species were mostly non-crystalline and consisted of sorbed mononuclear U(IV). A set of experiments was previously conducted in order to investigate the sensitivity of these U(IV) species to reoxidation [11]. This latter study indicated that oxidizing conditions slightly remobilized U after 8 days but bicarbonate addition highly increased U remobilization, even under reducing conditions[11]. Despite these results yielded a first insight in the reactivity of these sediments, the possible role of autochtonous microbial population on U(IV) remobilization processes was not investigated.

To date, the study of microbial cycling of U have been mostly focused on its interaction with bacteria [34-35]. However, a recent study reported a bioassociation between U and archaea species in rock salts in Germany [36]. Moreover, archaea species have already been identified nearby U polluted sites [37]. Among prokaryotes, archaea species are considered non-negligible in various environments, especially in soils and aquatic freshwater ecosystems, where they are estimated

to represent 2% [38] and 1% [39] of the microbial diversity, respectively. Their role on U reoxidation and especially upon reoxidation events by O_2 from fresh sediments is still largely unexplored.

The objective of the present study was to evaluate the influence of microbial communities on U reoxidation and mobilization from lake sediments during three-weeks long batch incubation experiments mimicking the first step of sediment dredging and surface storage operation. In the lake sediments studied, more than 85% of U is reduced in the form of mononuclear U(IV), which is representative of the speciation of U contaminated sediments [9,10,40,41,42]. Three different incubation conditions were investigated: full oxygenation that could occur under open-air surface repository conditions, anoxic conditions representing that would be expected under water-saturated conditions at the bottom of a storage pile, and 50% oxic conditions that may be the most relevant to storage sites. Our results indicate that intermediate oxidizing conditions (50% oxic) yielded the lowest U release rate even if mononuclear U(IV) was fully oxidized. According to the evolution of the physicochemical parameters of the incubation suspension (pH, alkalinity, $Fe^{2+}_{(aq)}$) and of microbial diversity, this results is interpreted as resulting from U(VI) scavenging by iron-oxyhydroxides resulting from microbial Fe(II) oxidation.

2. MATERIALS AND METHODS

2.1. Samples studied

Lake Saint Clément is located 20 km downstream from the former U mine of Bois Noirs/Limouzat in the Massif Central (France). It is supplied by the Besbre River, which is collecting the discharge of treated mine waters from the U mining site since its closure in 1980 (Figure S1). A sediment core of ~130-cm length was collected in August 2016 (46° 5’ 9’’ N, 3° 41’ 22’’ E) from a boat above the 12-meter-deep water column (at 120 meters upstream from the dam), using an Uwitec© gravity handcorer. Special care was given to the preservation of U

oxidation state by sealing the two core sections of 65-cm length into heat-sealed aluminized plastic films bags within an N_2-filled anoxic glove bag on the field. Core sections were then conditioned below 4°C for transportation to the laboratory where they were vacuum dried in an N_2-filled anoxic glove box (<5 ppm O_2). A previous study of the Lake Saint Clément sediments reported an increase of U concentration with depth, from 40 $mg.kg^{-1}$ at the top of the sedimentary column to 360 $mg.kg^{-1}$ at 180-cm depth [9]. For this study, sediment samples containing 195 to 233 $mg.kg^{-1}$ of U were selected from deep sediment layers, in which U is mainly present as mononuclear U(IV) and minor amounts of nano-crystalline U(IV)-phosphate [9]. These sediments are characterized by a high organic carbon content (8.5-12 wt% of total organic carbon), constant Si (around 20 wt%) and P content (0.17 wt%), Fe from 4 to 6-8 wt% and Ca from 0.37 to 0.55 wt% [10]. They mainly consists of quartz, feldspar, micas and chlorite, with traces of barite and pyrite [9]. Concentrations of dissolved nitrate and sulfide concentration in pore waters were below the detection limits of classical colorimetric methods suggesting that sulfide and nitrate were not key compounds of the U redox cycle in the sediments studied [10]. For our experiments, lake waters sampled at 12 m depth, i.e. close to the sediment-water interface, were collected using a Niskin bottle and used as incubation medium.

2.2. Experimental setup

The Lake water was filtered through a 0.22-µm filter and O_2 was removed via N_2-bubbling at 80°C during 1 hour. Once in a N_2-filled glove box, fresh anoxic sediments from the bottom of the core (112-117 cm depth) were mixed with the anoxic lake waters at a solid:liquid ratio of 1:10 under sterile conditions, using an electric burner. For each experimental condition, approximately 66 g of the lake water/sediment suspension was poured into a sterile flask.

For differentiating abiotic and biotic effects on U mobility, all three oxygenation conditions were performed either under biotic conditions using fresh sediments or under abiotic conditions

using sediments previously sterilized by gamma-irradiation as explained hereafter. Each condition was performed in triplicate. For abiotic experiments, the filled flasks were irradiated according to a ^{60}Co sealed source at a total absorbed dose rate of 30 ± 1.68 kGy (1.5 kGy per hour) at the Ionisos irradiation facility in Dagneux, France. This mode of sterilization was considered successful, with no viable cells counted in gamma-sterilized sediments at a total gamma-ray dosage of 20 kGy [43].

Incubations were conducted at room temperature under three distinct O_2 conditions: fully oxic "*100% O_2*" Erlenmeyer flasks agitated at 300 rpm, hypoxic "*50% O_2*" Erlenmeyer flasks agitated at 10 rpm, and anoxic "*0% O_2*" Erlenmeyer flasks agitated at 300 rpm inside N_2-filled anoxic glove box Jacomex® GPT3 (> 5 ppm). For all experiments each Erlenmeyer was closed with a sterile, air-permeable, cotton stopper. Dissolved oxygen was monitored weekly using a Multi 350i Set WTW® probe during the experiment and values were 8.52 ± 0.23 and 4.62 ± 0.66 mg/L for the *100% O_2* and *50% O_2* experiments, respectively. For the *0% O_2* experiments, a value of $2.82.10^{-5} \pm 6.84.10^{-6}$ mg/L dissolved oxygen was calculated using Henry's law, based on the pO_2 value measured in the anoxic glovebox atmosphere.

Suspension samples taken at starting point (Time = 0) and after 1, 2, and 3 weeks of incubation were filtered through a 0.22-µm pore-size cellulose filter. Colorimetric analyses of alkalinity [44] and of dissolved Fe^{2+} and Fe^{3+} [45] were performed immediately after filtration. Acidified (pH~1, HNO_3) and non-acidified aliquots were also stored at 4°C for further analyses of dissolved cations and anions, respectively. Dissolved U was determined using an ICP-MS 8800 Triple Quadrupole (Agilent). Relative standard deviation was below 10% as estimated from 5 measurements of the same sample, and limit of quantification was 0.03 $\mu g.L^{-1}$. Dissolved major cations were measured using an ICP-OES iCAP™ 7600 Duo (Thermo Fisher Scientific). Relative standard deviation was below 10% as estimated from 5 measurements of the same sample, and detection limits were 10, 100, 40, 100 and 30 $\mu g.L^{-1}$ for Fe, Ca, K, P and Si,

respectively. Total Dissolved Carbon (DC) was determined by measuring the CO_2 released after combustion at 850°C using a Carbon analyser (Vario TOC Cube analyzer, Elementar) equipped with a non-dispersive infra-red detector. Dissolved Organic Carbon (DOC) was estimated as DOC = DC - Alkalinity.

Starting sediment were analyzed as dry solid powders for Total Carbon (TC) using the same method as above. Total Organic Carbon (TOC) was also determined using the same method but the sample was acidified with a 1M HCl solution prior to combustion. The Total Inorganic Carbon (TIC) was then deduced from the difference between TC and TOC. Relative standard deviation was below 10% as estimated from 5 measurements of the same sample and limits of quantification were 0.019 and 0.05 ppm for solid TC and TOC respectively and 0.5 ppm for DOC.

2.3. XAS spectroscopy

X-ray Absorption Near-Edge Structure Spectroscopy (XANES) was used to determine U redox in the sediments before and after the incubation experiments. For this purpose, final solid samples were harvested by centrifugation after 3 weeks of incubation and vacuum dried in an N_2-filled anoxic glove-box. The collected sediments were vacuum dried in the same glove-box. All samples were ground in an agate mortar, pressed as 7 mm diameter pellets sealed between two layers of Kapton tape and mounted in Kapton-taped sample holders, in the same anoxic glove-box. They were then transported to the synchrotron facility within aluminized foil bags Protpack® sealed under anoxic atmosphere and placed into an anoxic plastic box containing a GasPak™. The sample bags were opened in an anoxic glove box at the beamline and samples were transferred inside the liquid N_2 cryostat, where they were placed under vacuum after N_2 purge of the sample chamber.

Eight samples were analyzed for XANES measurements at the U L_{III}-edge: 2 starting

samples (a non-irradiated and an irradiated fresh sediment) and 6 final samples, corresponding to fresh and irradiated sediments incubated for 3 weeks under the 3 different oxygen conditions. Data were collected in fluorescence detection mode using a 100-element solid state Ge array fluorescence detector at the high-flux 11-2 wiggler beam line of the Stanford Synchrotron Radiation Lightsource (SSRL, USA). The energy of the incident beam delivered by the Si(220) double-crystal monochromator was calibrated by setting the first inflection point of Y *K*-edge at 17038 eV, using a double transmission setup. Data were collected at 80K (liquid N_2 cryostat) in order to avoid photoreduction of U(VI) under the X-ray beam [46]. A minimum of 2 scans were collected for each sample, and series of up to 8 repeated scans on the same spot of selected samples indicated no redox change of U under beam exposure. XANES data were merged and normalized using the ATHENA code [47]. XANES spectra were fit using Linear Combination Least Square (LC-LS) of the spectra of our purest U(IV) and U(VI) species, namely U(IV)-citrate and U(VI)-pyrophosphate [9]. Using such a classical LC-LS procedure, determination of the U(IV) and U(VI) proportions rely both on the energy-shift in L_3-edge position between the two oxidation states (~2.7 eV) and on the characteristic shoulder in the XANES spectrum of the uranyl ion $U^{VI}O_2^{2+}$ [6-11]. The fit were performed with a home-built code [9,48] based on Levenberg-Marqardt minimization algorithm. The quality of the LC-LS fits was estimated by a R-factor: $Rf = \Sigma [\mu_{exp} - \mu_{calc}]^2 / \Sigma \mu_{exp}^2$ where μ is the normalized absorbance. The uncertainty on XANES LC-LS fitting components was estimated by $3 \times \sqrt{3 \sqrt{}}[VAR(p). \chi^2_R]$ (Ravel and Newville, 2005), where $VAR(p)$ is the variance of component p for the lowest χ^2_R value; with $\chi^2_R = N / (N-N_p) \sum [\mu_{exp} - \mu_{calc}]^2$, where N_p is the number of fitting components and N is the number of independent parameters. N was calculated as the energy range divided by the natural width of the U L_{III} [49].

2.4. Microbial analyses and bioinformatics

Total genomic DNA was extracted from 3 independent samples of fresh sediments in initial conditions as well as after 3 weeks incubation under contrasted oxygenation conditions (*0% O_2*, *50% O_2* and *100% O_2*). Amplicons of the V4 region were sequenced and a total of 9.070.946 paired-end reads (with a mean read length of 243 bases) were generated through Illumina MiSeq sequencing. Initial fresh sediments and those sampled after 3 weeks of incubation were separated by centrifugation (20 minutes at 6000 and 8500 rpm in the glove box and under oxidizing conditions respectively). DNA was extracted from pellets using the Powersoil DNA isolation kit Mobio on triplicate samples per incubation condition. Purified DNA was quantified by fluorescence using the Picogreen DNA quantification kit (Invitrogen). Libraries, sequencing and data analysis described in this section were performed by Microsynth AG (Balgach, Switzerland).

To sequence the V4 regions of the bacterial 16S rRNA gene, two-step Nextera PCR libraries using the primer pair 515F (5′-GTG CCA GCM GCC GCG GTA A -3′) and 806R (5′- GGA CTA CHV GGG TWT CTA AT-3′) were created [50]. Subsequently the Illumina MiSeq platform and a v2 500 cycles kit were used to sequence the PCR libraries. The produced paired-end reads which passed Illumina's chastity filter were subject to de-multiplexing and trimming of Illumina adaptor residuals using Illumina's real time analysis software included in the MiSeq reporter software v2.6 (no further refinement or selection). The quality of the reads was checked with the software FastQC version 0.11.7 [51]. The locus specific V4 primers were trimmed from the sequencing reads with the software cutadapt v1.18 [52]. Paired-end reads were discarded if the primer could not be trimmed. Trimmed forward and reverse reads of each paired-end read were merged to *in-silico* reform the sequenced molecule considering a minimum overlap of 15 bases using the software USEARCH version 11.0.667 [53]. Merged sequences were then quality

filtered allowing a maximum of one expected error per merged read. Reads that contain ambiguous bases or are outliers regarding the amplicon size distribution are also discarded. The remaining reads were denoised using the UNOISE algorithm implemented in USEARCH to form operational taxonomic units (OTUs) discarding singletons and chimeras in the process. The resulting OTU abundance table is then filtered for possible bleed-in contaminations using the UNCROSS algorithm and abundances are adjusted for 16S copy numbers using the UNBIAS algorithm. OTUs were compared against the reference sequences of the RDP 16S database [54] and taxonomies were predicted considering a minimum confidence threshold of 0.7 using the SINTAX algorithm implemented in USEARCH. Alpha diversity was estimated using the Richness (Observed), Chao1 and Shannon indexes. Beta diversity was calculated using the weighted Unifrac distance method [55] on basis of rarefied OTU abundance counts per sample. Alpha and beta diversity calculations and the rarefaction analysis were performed with the R software packages phyloseq v1.22.3 and vegan v2.5-1. To detect differentially abundant OTUs depending on collected sample metadata (e.g., medication, environmental conditions), differential OTU analysis on normalized abundance counts was performed with the R software package DESeq2 v1.18.1 [56].

To reveal inter-sample relations, non-metric multidimensional scaling (NMDS) based on the Bray-Curtis dissimilarity (k=3) was performed. A permutational multivariate analysis of variance (PERMANOVA) was also performed, with 999 permutations using the *adonis* function of the *Vegan* R package.. Venn diagram and heat maps were produced using respectively the *venn* and *heatmap.2* functions from the *gplots* R package [58]. The selection of the 30 most abundant OTUs was based on raw abundances, whereas log10-transformed abundances (log10(1+x)) are shown on heat maps. Sequences were registrated under accession number PRJNA669547 in the SRA database of NCBI.

Richness and diversity estimates were calculated (Table S1). The Chao1 estimator indicated good coverage of OTU, richness throughout and asymptotic rarefaction curves analysis for all samples (Figure S4) revealed that the overall prokaryotic diversity was well represented. Specific richness and evenness were expressed by the Shannon index. The highest diversity was observed in the initial sample, whereas incubation conditions reduced the diversity. *0% O_2* and *100% O_2* conditions revealed lower diversities, in contrast, the *50% O_2* condition presented the closest Shannon index value to the one observed in initial conditions (Table S1).

3. RESULTS

3.1. Evolution of solution chemistry in the incubation experiments

The chemical composition of the filtered supernatant solutions was followed over the course of the incubation experiments, by measuring dissolved U (Figure 1), pH and alkalinity (Figure 2), dissolved organic carbon (Figure S2) as well as total dissolved Fe and Fe^{2+}. (Figure 3). Other major elements including Ca, K, P and Si were also measured, as reported in Figure S3.

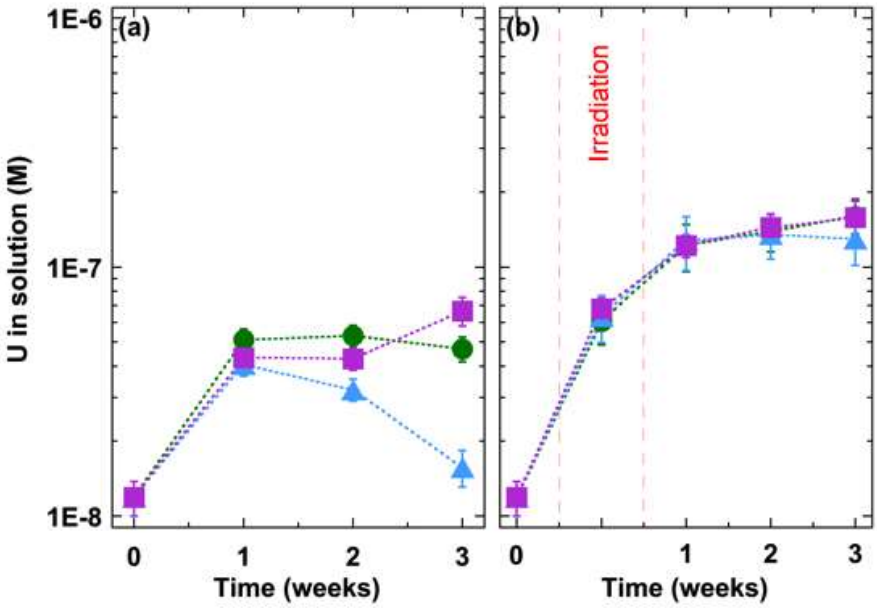

Fig. 1 Uranium mobilization for (a) non-irradiated and (b) irradiated sediments, throughout 3-week incubation under different O_2 conditions: ● *100% O_2* incubation; ▲ *50% O_2* incubation; (■, *0% O_2*. Error bars represent the standard deviation over the 3 replicates for each condition.

For the non-irradiated sediments (Figure 1a) the amount of dissolved U, released over time in the incubation supernatant differed with the oxygenation conditions, whereas it did not vary with the oxygenation conditions for the irradiated sediments (Figure 1b). More precisely, for the non-irradiated sediment (Figure 1a), under *100% O_2*, dissolved U increased and stabilized until the third week. Under *50% O_2*, U release was followed by a decrease in dissolved U concentration. Finally, under *0% O_2*, the release of U increased all along the experiment. For the irradiated sediments (Figure 1b), the dissolved U concentration increased over time, following a same pattern under the three oxygenation conditions, and the U release was overall higher than for the non-irradiated sediments.

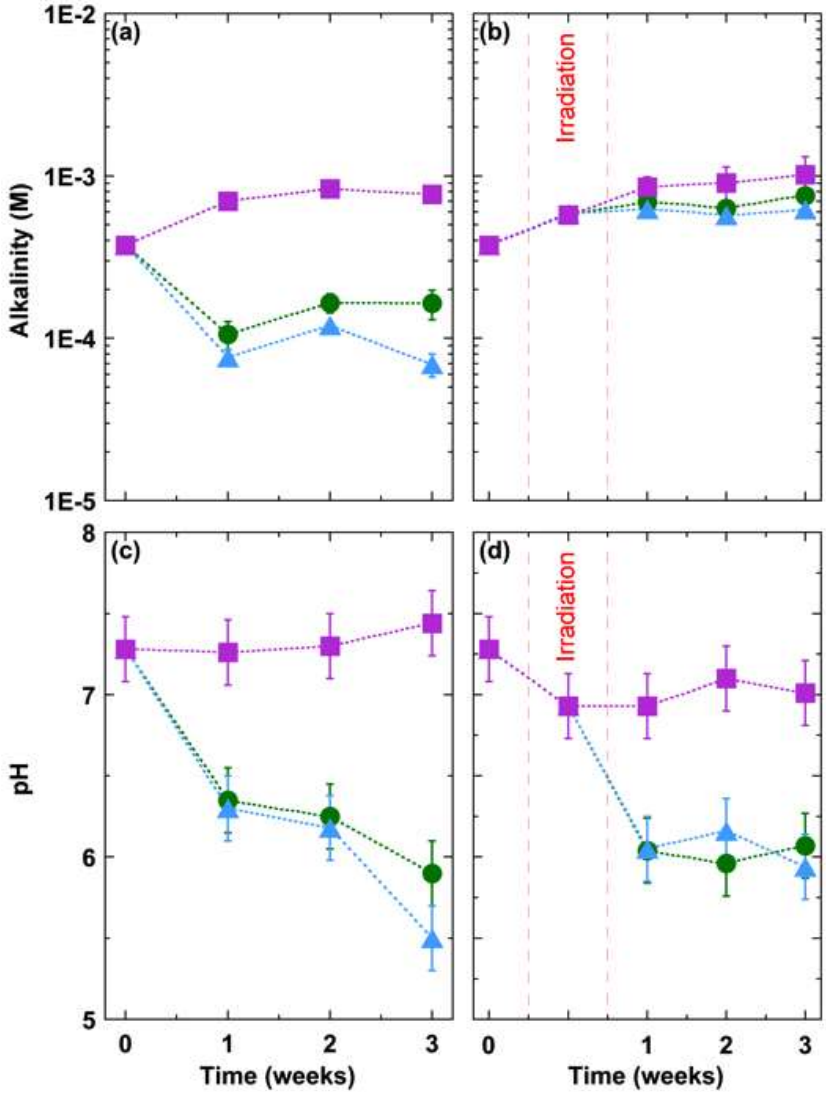

Fig. 2 Alkalinity and pH for (a, c) fresh and (b, d) irradiated sediments, throughout 3-week incubation under different O_2 conditions: ● *100% O_2* ; ▲ *50% O_2* ; ■ *0% O_2*. Error bars represent the standard deviation over the 3 replicates for each condition.

Alkalinity was found to increase with time in all experiments except in the *50% O_2* and *100% O_2* experiments conducted with the non-irradiated sediments (Figure 2a and b). The increase in alkalinity is interpreted as resulting from an increase in the buffering capacity of the solution, which could be explained by the progressive release of alkaline and alkaline-earth cations (Figure S3), as well as the release of aqueous Fe^{2+} (Figure 3a,b) in the anoxic incubations. The pH remained neutral under *0% O_2* conditions, whereas it significantly dropped over incubation time under 5*0 and 100% O_2* conditions (Figure 2 c,d), down to pH 5.5 for biotic *50% O_2*

conditions. Aqueous H_2CO_3 concentrations calculated from measured alkalinity and pH values (Figure 2) were found to be in the range of $4.15\ 10^{-5}$ to $1.69\ 10^{-3}$ M, thus in excess with respect to the value expected for equilibrium with atmospheric CO_2 ($[H_2CO_{3aq}] = 1.41\ 10^{-5}$M). This result suggests that our incubation media did not fully degassed the CO_2 produced by the pH drop, which could be related to the cotton stopper of the Erlenmeyer vessels that were used.

Interestingly, it is expected that the observed pH decrease (Fig. 2c,d) was caused by Fe(II) oxidation under oxygenation conditions (Fig. 3). Under fully anoxic conditions (*0% O_2)*, total dissolved Fe concentrations were the highest and Fe was mainly released in the first week of incubation, essentially in the form of Fe(II), the same trend being observed for non-irradiated and irradiated samples (Figure 3). In contrast, under *100% O_2* conditions, approximately half of the initial dissolved Fe was progressively removed from the solution and this Fe removal was even more pronounced under *50% O_2* conditions. Abiotic experiments exhibited a similar behaviour but with less pronounced Fe removal under *50% O_2* conditions. The decrease of total Fe observed in the presence of oxygen, can be partly explained by the removal of Fe(II) (Figure 3c,d), which suggests Fe(II) oxidation and subsequent precipitation of iron oxides, well known as resulting in an acidification of the medium.

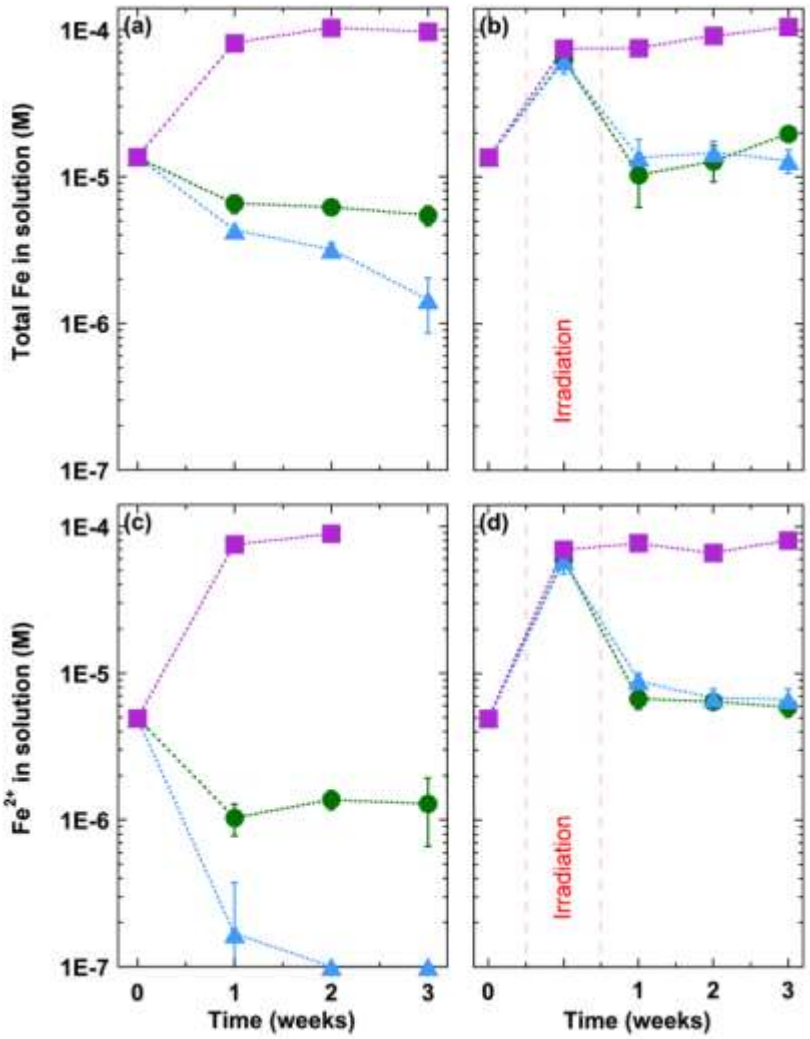

Fig. 3 Total Iron in solution and Fe^{2+} in solution for (a, c) fresh and (b, d) irradiated sediments. Measures during 3 weeks of incubation under different O_2 conditions: green circles (●), *100% O_2* incubation; blue triangles (▲), *50% O_2* incubation and purple squares (■), *0% O_2* incubation. Error bars represent the standard deviation over the 3 replicates for each condition.

The above-mentioned results regarding the solution chemistry led us to infer that microaerophilic conditions are the most favourable conditions for decreasing U remobilization from the lacustrine sediments. The removal of both dissolved U (Figure 1) and Fe(II) (Figure 3) under biotic hypoxic conditions especially suggested that Fe oxidation could have limited U release under these conditions, which is further discussed thereafter.

3.2. Evolution of solid U oxidation state

U oxidation state was assessed using XANES spectroscopy in the solid phase of fresh and irradiated sediments at the start of the experiments and after 3 weeks of incubation (Figure 3; Table S2).

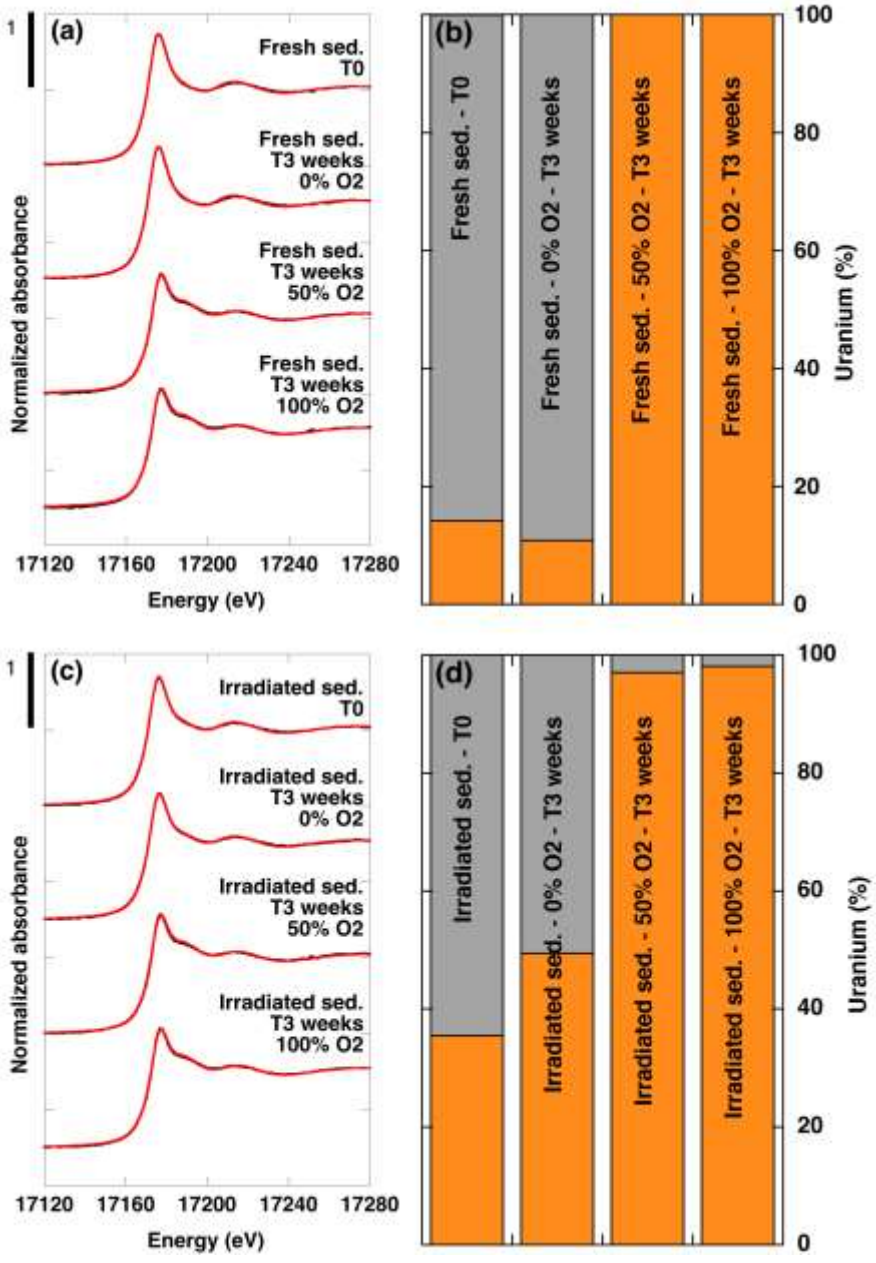

Fig. 4: U L_{III}-edge XANES experimental data (black) and fit (red) and the corresponding proportions of U(IV) (grey) and U(VI) (orange) for (a, b) fresh sediments and (c, d) irradiated sediments. XANES LC-LS fitting components are reported in Table S2.

In unreacted non-irradiated sediments (Figure 3a,b), U was mostly in the U(IV) form (~86% of total U) and remained in this reduced form (~89% of total U) after 3 weeks under anoxic conditions (i. e. *0% O_2*). In contrast, U was ~100% U(VI) after 3 weeks under hypoxic and fully oxic conditions (i. e. *50% O_2* and *100% O_2*) (Table S2).

The gamma-sterilization procedure was found to induce a partial oxidation of U, with U(IV) decreasing from ~86 to ~65% (Figure 3c,d). The redox state of U remained then unchanged after 3 weeks under reducing conditions. In contrast, both under *50%* and *100% O_2* conditions, U was fully oxidized after 3 weeks.

These results indicate that our hypoxic conditions (50% O_2) were sufficient to fully oxidize U(IV) to U(VI) in the lacustrine sediments studied. In order to determine the influence of solution chemistry on U remobilization, including especially the effect of bicarbonate ions, U aqueous speciation was calculated using thermodynamic equilibrium approach, as detailed in the following section.

3.3. Uranium aqueous speciation at the end of the incubations

The final distribution of dissolved U species (Figure 5, Tables S3, S4, S5) was calculated with the geochemical code Phreeqc [59] using the chemical composition of the aqueous phase at the end of each experiment (Figures 1, 2, 3, 5). Chemical reaction taken into account in our model are listed in (Table S3) together with corresponding thermodynamic equilibrium constants, as taken from WATEQ4F database [59]. According to these calculations, U was expected to be mainly in the form of aqueous U(VI)-carbonate complexes at the end of the *50% O_2* and *100% O_2* experiments, with UO_2CO_3 and, to a lesser extent, $UO_2(CO_3)_2^{2-}$ complexes as major species (Figure 5). This result is consistent with the well-known affinity of U(VI) for aqueous carbonate species, which results in the formation of a variety of soluble U(VI)-

carbonato complexes at near neutral and alkaline pH (Clark et al., 1995). A previous study on the same sediments indicated the importance of this process in U release under alkaline conditions (Seder-Colomina et al., 2018). For the *0% O_2* experiments, aqueous U was also calculated to be present as aqueous U(VI)-carbonate complexes, in the form of $CaUO_2(CO_3)_3^{2-}$ (71.9 and 45.2%) and, to a lesser extent, $UO_2(CO_3)_2^{2-}$ (7.7 and 30.6%) for non-irradiated and irradiated sediments, respectively (Figure 4). In these anoxic experiments, a minor fraction of dissolved U (11-18%) was calculated to be under the U(IV) form, complexed to dissolved organic matter (Figure 5). Moreover, 3 to 5% of U(VI) associated to humate was found for all the irradiated sediments. These results suggested an important role of U(VI) complexation by carbonates as a driver for U mobilization from the sediments, including in the anoxic incubation experiments.

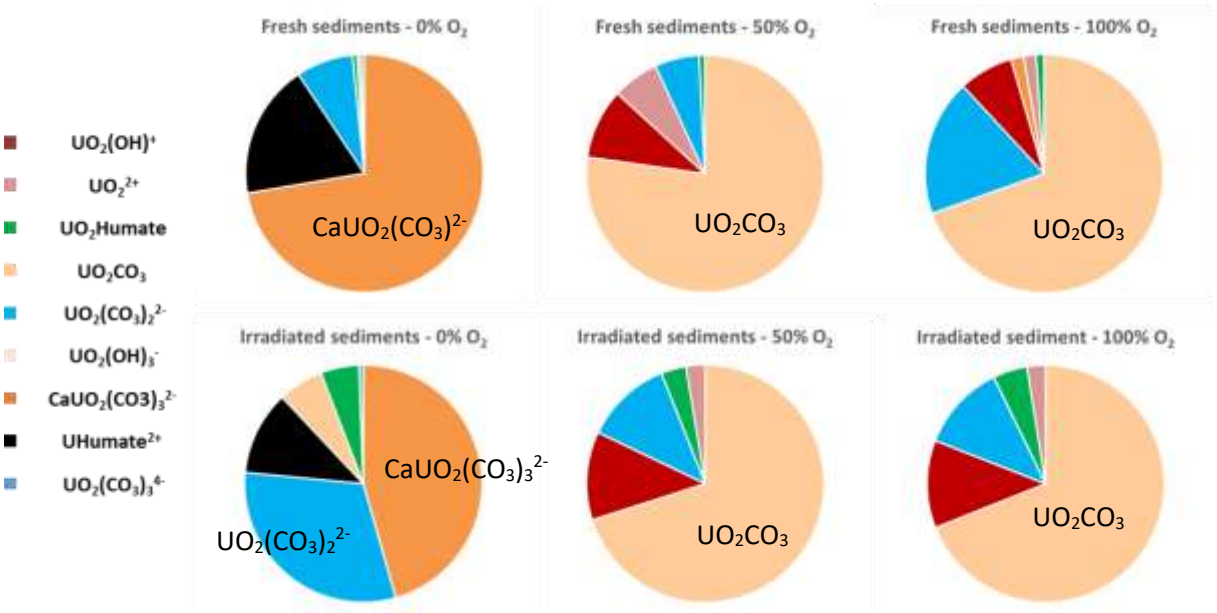

Fig. 5 Equilibrium calculations of dissolved uranium speciation at the end of each experiment. Calculation were conducted with Phreeqc [59] using the chemical composition of the aqueous phase at the end of each experiment (Table S4 and S5). Redox conditions were considered to be controlled by dissolved oxygen for the *50% O_2* and *100% O_2* experiments and by aqueous Fe^{2+} for the *0% O_2* experiments.

3.4. Evolution of microbial communities of the sediments in the incubation

Considering the global analysis of the dataset, NMDS plot revealed that both oxic conditions (*100% O_2* and *50% O_2* samples) exhibited the greatest sample variation and clustered closely together (Figure S5). A permutation test confirmed that the redox conditions of exposition explained most of the variance (R^2 of 0.96, *p*-value of 0.001). Most OTUs (1144 among 1214) are detected regardless of the experimental conditions (Figure 6A). Remaining OTUs are specific to oxygenation conditions. Few OTUs, which were not detected in initial sediments, were detected after 3 weeks incubation in controlled oxygen conditions.

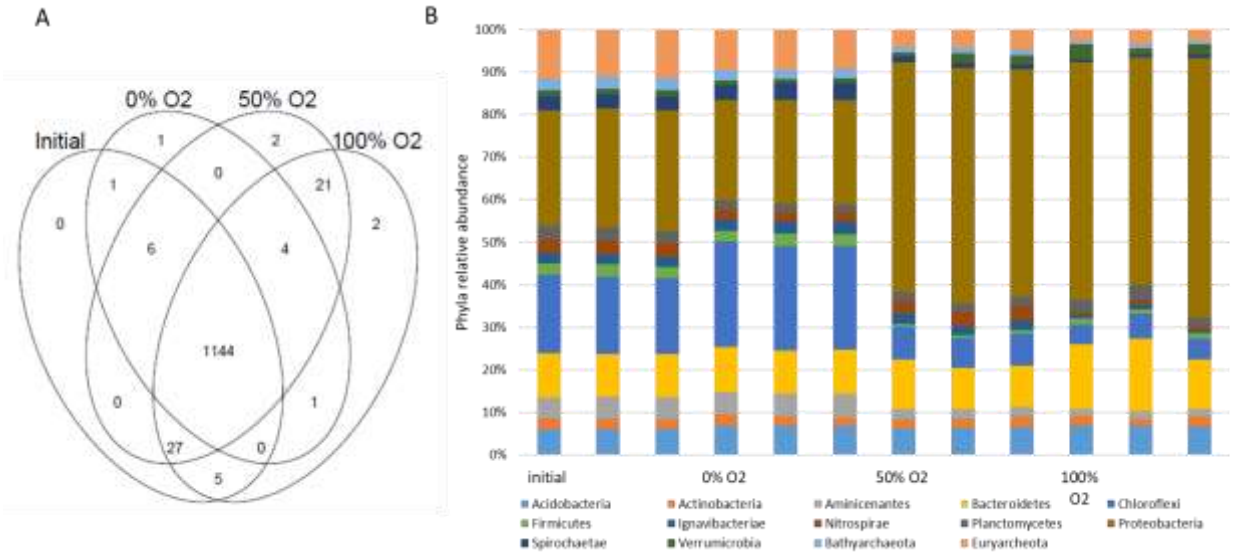

Fig. 6 A: Venn diagram of OTU repartition showing the overlap of the prokaryotic community for the initial sediments and after 3 weeks of incubation under different O_2 conditions (*100% O_2*, *50% O_2* and *0% O_2* samples). B: Relative abundance of OTUs at the phyla level for the initial sediments and after 3 weeks of incubation under different O_2 conditions. Phyla corresponding to more than 1% abundance are considered.

Relative abundances of phyla greater than 1% are close in the initial sediment and in sediment incubated in anoxia for 3 weeks. Likewise, close relative abundances are observed under oxic and hypoxic incubation conditions (Figure 6B). Proteobacteria are also favored

under oxic and hypoxic conditions, while the bacterial phyla *Chloroflexi*, *Firmicutes* *Aminicenantes*, *Spirochaetes* are less abundant as well as the Archaea phyla of *Euryarcheota* and *Bathyarcheota*. As expected, these results confirm that oxygenation is a strong structuring factor of prokaryotic communities in our incubation conditions.

Since microaerophilic conditions were shown the most favourable conditions for decreasing U remobilization from the lacustrine sediments, Figure 7 shows the 30 most abundant OTUs after 3 weeks of incubation under hypoxic conditions (similar data for initial sediment, fully oxic and anoxic conditions are given figure S6). OTU 4 corresponding to *Thiobacillus* is present everywhere but dominates in oxic conditions. However, considering *50% O_2* incubation condition, 3 OTUs appear specifically dominant in this condition. One (OTU 115) is affiliated to nitrosomodale (0.7379) and to Gallionellaceae (0.69) a family containing ferrous iron - oxidizing bacteria [60-61], already noticed in prototype 19 in the network analysis. The second (OTU 85) belongs to Hydrogenophilale order which contains only one family and two genus : *Hydrogenophilus*, known as thermophile, but the existence of non thermophilic strains is probable because DNA of *Hydrogenophilus thermoluteolus* was detected in ice core samples [62], and *Thiobacillus* corresponding to sulphur oxidizing bacteria. The last one (OTU 29) is affiliated to candidatus *Odyssella* genus, whose type species was described as an obligate intracellular parasite of *Acanthamoeba sp.* [63], a group of amoeba forming cysts under anoxic conditions, able of revival under oxygenated conditions [64] and sensitive to high oxygen concentration[65].

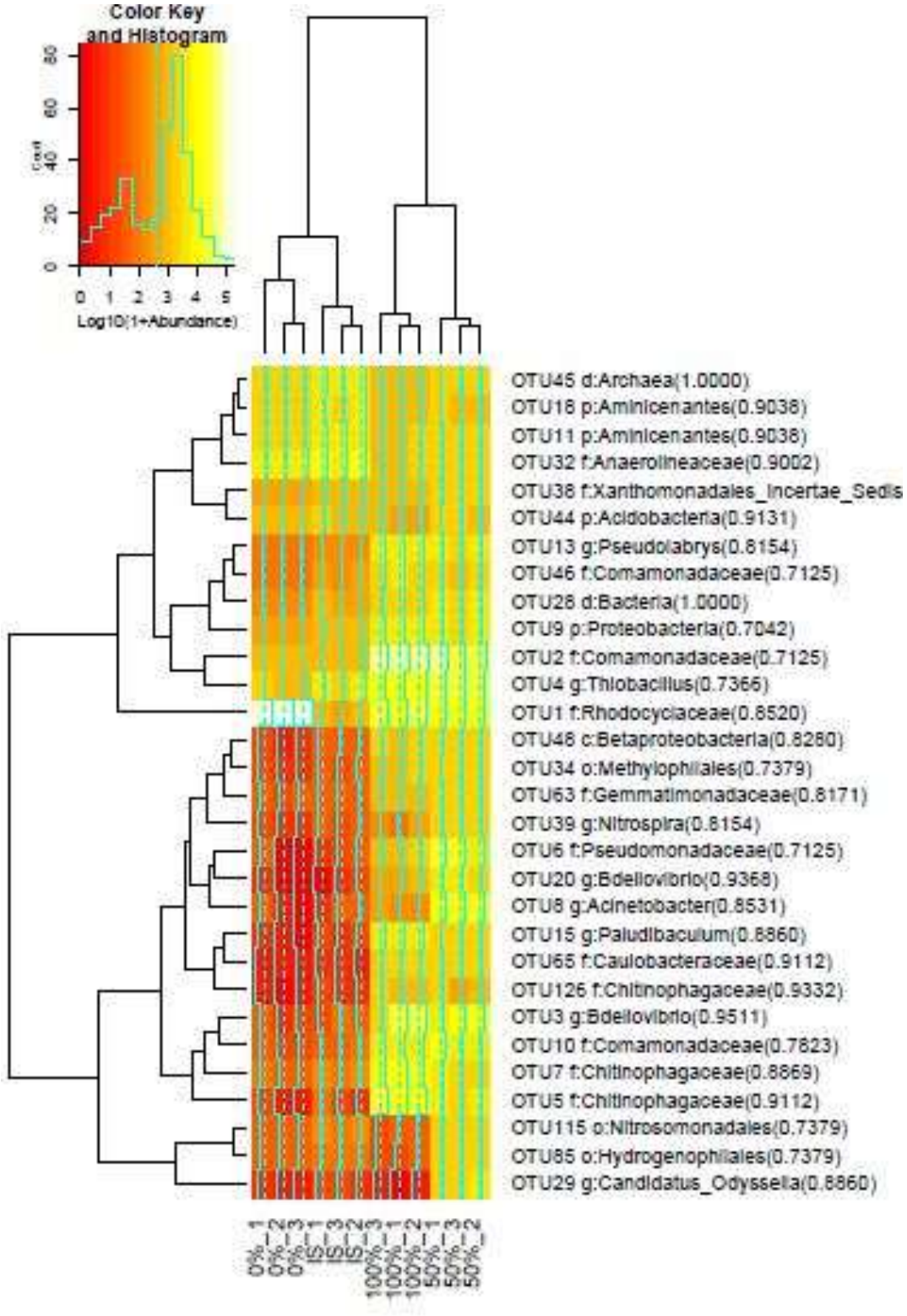

Fig. 7 Heat map and hierarchical cluster analysis of log-transformed abundances of the 30 most abundant OTUs (based on raw abundances under hypoxic conditions) after 3 weeks of incubation. The dendrogram represents complete linkage clustering. Assignments after OTUs numbers give the lowest taxonomic level associated with the OTU using the silva database k: kingdom, p: phylum, o: order, f: family, s: genus_species. Values in brackets indicate sequence similarity.

4. DISCUSSION

4.1. Effect of oxygenation and mechanism of U release

XANES results indicate that oxygenation lead to U(IV) oxidation to U(VI) in the solid phase and geochemical modelling indicated the formation of aqueous U(VI)-carbonato complexes leading to U release from the sediments. Moreover, even under anoxic conditions in which solid U(IV) was largely preserved, the formation of aqueous U(VI)-carbonato complexes shifts the U-redox couple equilibrium and also lead to U release[11,17,67]. In addition, the results of our biotic incubation experiments suggest that the oxygenation level of the incubation medium exerted a pivotal control on U mobilization rates from lake sediments, the lowest U release being observed under hypoxic conditions. In contrast, for abiotic experiments, the U release was higher and unaffected by the oxygenation level. The absence of an oxygenation effect for sterilized samples suggested that microbial activity could have been involved in the U removal under biotic conditions. The removal of U at the end of the hypoxic incubation was accompanied a drop in pH, alkalinity and dissolved Fe(II), which deserves to be interpreted under the light of the observed evolution of chemical and biological parameters during the incubation.

4.2. Effect of iron oxidation on alkalinity and pH

Aqueous U-carbonate complexes are favoured under alkaline conditions and are known to stabilize aqueous U(VI) against solid U(IV) species, which may thus facilitate the oxidation and dissolution of solid U(IV) species, even under anoxic conditions [6,11,17,66]. Conversely, the decrease in alkalinity and pH observed in our biotic *50% O_2* and *100% O_2* incubations (Figure 2a) may explain the limitation of U release (Figure 1) compared to more alkaline conditions

observed in our biotic *0%* O_2 incubations. This decrease in alkalinity observed under oxic and hypoxic conditions could be explained by the oxidation of aqueous Fe^{2+}, followed possibly by its precipitation as Fe^{3+} oxyhydroxides, as suggested by the removal of aqueous Fe^{2+} during these incubation experiments (Figure 3c). Ferric oxyhydroxide precipitation generates two H^+ ions for each oxidized Fe^{2+} ion and could thus explain the pH drop, while Fe^{2+} removal could explain the alkalinity drop (Figure 3c). Then, the acidification of the solution might have displaced the H_2CO_{3aq} / $HCO_3^-{}_{aq}$ equilibrium, which generated an excess of H_2CO_{3aq}. We suggest that CO_{2gas} degassing did then not reach equilibrium with atmosphere due to the use of air-permeable cotton stopper to close the Erlenmeyer flask, which have resulted in an accumulation of CO_2 in the lower section of the head-space and in solution, thus maintaining a low pH. Although not ideal, these conditions may be viewed as a semi-closed carbonate system that could however be considered as representative of confined conditions in a sub-surface storage site. These conditions may have limited aqueous complexation of U(VI) by bicarbonate ions and could also have favoured U adsorption onto ferric-oxyhydroxides, which deserves further discussion.

4.3. Effect of iron oxidation on U immobilization

The efficient removal of dissolved Fe(II) observed under biotic hypoxic conditions contrasts with the low Fe(II) removal observed for the other conditions, especially abiotic ones (Figure 3). Low oxygen concentrations such as those encountered under microaerophilic conditions are favourable to bacterial Fe(II) oxidation instead of fast and spontaneous abiotic reaction [67-68], which suggest that microbial process could be involved in the higher removal of Fe(II) under biotic hypoxic conditions (Figure 3c). Microbial Fe(II) oxidation is known to induce the formation of biogenic Fe(III) oxyhydroxides, frequently in the form of ferrihydrite and

lepidocrocite, with possible sequestration and/or nucleation of theses phases within the biofilm [60,69-72]. Biogenic ferrihydrite is especially effective for sorbing U(VI) [73-76]and could thus have contributed to the limitation of U release in our hypoxic biotic incubation experiments. It is noteworthy, albeit abiotic oxidation of aqueous Fe^{2+} and ferric oxyhydroxides precipitation likely occurred in our fully oxic biotic incubations, U was not removed from the solution, which reinforce the possible role of microbial processes in U retention observed under hypoxic conditions. Moreover, Fe(III) photoreduction previously identified in natural sediments [79] could be another process which lead to the limited Fe(II) oxidation under fully oxidizing conditions.

4.4 Influence of microbial communities on uranium mobility

The observed microbial population dynamics suggested that hypoxic conditions have favoured microaerophilic microbial populations. Indeed, these conditions revealed that OTU's assigned to *Gallionellaceae* family were identified and described as a neutrophilic Fe oxidizer family [60-61]. Two other OTU's identified under these conditions were known to be capable to i/ dissimilatory Fe(III) reduction (OTU 15 - *Paludibaculum* genus) (Figure 7) and related to ii/ a Fe oxidizing family (OTU 115 - *Gallionellaceae* genus). Moreover, the predominance of *Thiobacillus* genus under oxic conditions is an important result. This genus corresponds to facultative anaerobiobligate chemolithotrophs using reduced sulphur compounds as energy source. Indeed, acidophilic Fe oxidative bacteria were described in this genus, such as *Thiobacillus ferrooxidans* and *Thiobacillus prosperus* but were then reclassified in other genera [61,78]. Interestingly, *Thiobacillus denitrificans* is particularly notable for its ability to oxidize sulfur and U compounds in a nitrate-dependent manner [79].

The particular abundance of this genus observed under microaerophilic conditions makes it a potential actor of efficient of sulphur or Fe or U oxidation in these conditions. Moreover, the

specific abundance of OTU 115 identified could support our hypothesis of biologically mediated Fe oxidation that could explain the lower pH and the lower U mobilization observed under microaerophilic conditions. Its specific role needs to be further explored.

4.5 Effect of gamma-sterilization on uranium reactivity

Uranium release was observed to be higher in abiotic than in biotic conditions, with no influence of oxygenation conditions on the removal of U from the sterilized sediments. This behavior suggested a possible effect of the sterilization method as enhancing U mobility. Partial oxidation of U(IV) to U(VI) immediately after gamma-sterilization, under anoxic conditions, could be related to the formation of reactive oxygen species, for instance from water radiolysis, that could be able to oxidize U [17]. Although the actual mechanism and the identity of the U oxidized species remained not elucidated in the present study, irradiation prior to incubation appeared to favour the lability of U regardless the redox conditions (Figure 1b). However, solid U reoxidation was incomplete with minute amounts of residual U(IV), likely in the form of less reactive nanocrystalline U(IV)-phosphate[9] and/or as inaccessible U in metamictic zircon and monazite crystals identified previously in the sediments [9,10]. The increased U mobilization from the irradiated sediments could be explained by the higher U(VI) proportion than in the non-irradiated ones, at the start of the incubations (Figure 2). This mode of sterilization was also previously shown to favor U remobilization in oxidizing laboratory incubations [81], which was explained by the leaching of dead microbial cells and the release of DOC. In addition, the absence of microbial activity seems to have limited Fe^{2+} oxidation and removal of U under hypoxic conditions, by contrast with the higher Fe^{2+} removal (Figure 3) and pH drop (Figure 2) observed under biotic conditions, and which accompanied U removal from solution (Figure 1).

4.6 Environmental implications

The present study evidenced the potential role of microorganisms for minimizing the release of U under oxidizing conditions that can be encountered after sediment dredging operations. These results revealed that U sequestration in the sediment solid phase could be especially favored under confined hypoxic conditions that enhance microbial Fe^{2+} oxidation. Indeed, ferrous iron oxidation followed by ferric-oxyhydroxides precipitation lowers the pH and alkalinity of the solution, which reduces the amount of available carbonate ligands available for U(VI) mobilization. In addition, ferric-oxyhydroxides may sorb U(VI) and again limit its mobility. Such a role of biogenic ferric-oxyhydroxides in U(VI) scavenging during reoxidation of U(IV)-contaminated sediments is consistent with previous laboratory incubation conducted on shallow groundwater sediments spiked with biogenic UO_2[74]. Here we show that biogenic iron oxidation may limit U mobility during the reoxidation of genuine U-contaminated sediments, carefully sampled under anoxic conditions in a mining-impacted lacustrine environment. Hence, in our hypoxic experiment, dissolved U concentration ended up at only 3.6 $\mu g.L^{-1}$ after three weeks of incubation at a solid-solution ratio of 1:10. Under fully oxic or anoxic conditions, U remobilization was higher but did not exceed 8.3 and 15 $\mu g.L^{-1}$, respectively. This low U mobility contrast with the results of a previous study that have addressed U remobilization from the same sediments in the presence of high bicarbonate concentrations at pH value reaching ~9.5 [11]. In this latter study, the U release was up to 40 to 100 times higher at pH 8.5 to pH 9.5, due to U(VI) complexation to aqueous carbonate ions.

Our results show that oxygen can exert a strong control on the microbial community structure, which can significantly influence the mobility of U. However, although oxygen is generally assumed to favor U(IV) to U(VI) oxidation and release especially under acidic conditions[82], our results suggest that more complex interactions occur under neutral pH

conditions, in which ferric iron is insoluble, which might be important to consider for evaluating contaminated sediments management practices. More precisely our results suggests that U(VI) mobilization from sediments could be limited by bacterial Fe(II) oxidizing activity under hypoxic conditions. Further research would be however needed to assess the efficiency of such a biogeochemical process under dynamic conditions constrained by seasonal fluxes of meteoric waters.

ACKNOWLEDGMENTS

This work was partially supported by the CNRS federator project Needs Environnement and by IRSN. We thank EDF and DREAL Rhône-Alpes Auvergne for having authorized access to the lake of Saint-Clément. The SSRL facilities are acknowledged for having provided beamtime. SSRL and SLAC are supported by the U.S. Department of Energy (DOE), Office of Science, Office of Basic Energy Sciences under Contract No. DE-AC02-76SF00515, the DOE Office of Biological & Environmental Research, and by the National Institutes of Health, National Institute of General Medical Sciences (including P41GM103393). Partial support was provided by the U.S. DOE BER and SBR program.

APPENDIX A. SUPPLEMENTARY DATA

REFERENCES

1. D. Brugge, L. J. de Lemos,, B. Oldmixon, Exposure pathways and health effects associated with chemical and radiological toxicity of natural uranium. Rev. Env. Health., 2005, 20, 177-194.
2. IRSN, MIMAUSA database website (https://mimausabdd.irsn.fr/), accessed 4 February 2022.

3. Y. Wang, M. Frutschi, E. Suvorova, V. Phrommavanh, M. Descostes, A. A. A. Osman, G. Geipel, R. Bernier-Latmani, Mobile uranium(IV)-bearing colloids in a mining-impacted wetland, Nat. Commun., 2013, 4, 2942.
4. C. Mikutta, P. Langner, J. R. Bargar, R. Kretzschmar, Tetra- and Hexavalent uranium forms bidendate-mononuclear complexes with particulate organic matter in a naturally uranium-enriched peatland, Environ. Sci. Technol., 2016, 50, 10465–10475.
5. A. Mangeret, P. Blanchart, G. Alcalde, X. Amet, C. Cazala, M.-O. Gallerand, An evidence of chemically and physically mediated migration of 238U and its daughter isotopes in the vicinity of a former uranium mine, J. Environ. Radioact., 2018, 195, 67–71.
6. L. Stetten, P. Blanchart, A. Mangeret, P. Lefebvre, P. Le Pape, J. Brest, P. Merrot, A. Julien, O. Proux, S. Webb, J. R. Bargar, C. Cazala, G. Morin, Redox Fluctuations and Organic Complexation Govern Uranium Redistribution from U(IV)-Phosphate Minerals in a Mining-Polluted Wetland Soil, Brittany, France, Environ. Sci. Technol., 2018a, 52, 13099–13109.
7. L. Stetten, P. Lefebvre, P. Le Pape, A. Mangeret, P. Blanchart, P. Merrot, J. Brest, A. Julien, J. R. Bargar, C. Cazala, G. Morin, Experimental redox transformations of uranium phosphate minerals and mononuclear species in a contaminated wetland, J. Hazard. Mater., 2020, 121362.
8. V. Noël, K. Boye, J. S. Lezama Pacheco, S. E. Bone, N. Janot, E. Cardarelli, K. Williams, J. R. Bargar, Redox Controls over the Stability of U(IV) in Floodplains of the Upper Colorado River Basin, Environ. Sci. Technol., 2017, 51, 10954–10964.
9. G. Morin, A. Mangeret, G. Othmane, L. Stetten, M. Seder-Colomina, J. Brest, G. Ona-Nguema, S. Bassot, C. Courbet, J. Guillevic, Mononuclear U (IV) complexes and ningyoite as major uranium species in lake sediments, Geochem. Perspect. Lett., 2016, 2, 95–105.
10. L. Stetten, A. Mangeret, J. Brest, M. Seder-Colomina, P. Le Pape, M. Ikogou, N. Zeyen, A. Thouvenot, A. Julien, G. Alcalde, J. L. Reyss, B. Bombled, C. Rabouille, L. Olivi, O. Proux, C. Cazala, G. Morin, Geochemical control on the reduction of U(VI) to mononuclear U(IV) species in lacustrine sediments, Geochim. Cosmochim. Acta, 2018b, 222, 171–186.
11. M. Seder-Colomina, A. Mangeret, L. Stetten, P. Merrot, O. Diez, A. Julien, E. Barker, A. Thouvenot, J. R. Bargar, C. Cazala, G. Morin, Carbonate Facilitated Mobilization of Uranium

from Lacustrine Sediments under Anoxic Conditions, Environ. Sci. Technol., 2018, 52, 9615–9624.

12. H., Foerstendorf, K. Heim, A. Rossberg, The complexation of uranium(VI) and atmospherically derived CO_2 at the ferrihydrite–water interface probed by time-resolved vibrational spectroscopy. J. Colloid Interface Sci., 2012, 377, 299–306.
13. L. N. Moyes, R. H. Parkman, J. M. Charnock, D. J. Vaughan, F. R. Livens, C. R. Hughes, A. Braithwaite, Uranium Uptake from Aqueous Solution by Interaction with Goethite, Lepidocrocite, Muscovite, and Mackinawite: An X-ray Absorption Spectroscopy Study, Environ. Sci. Technol., 2000, 34, 1062–1068.
14. D. Langmuir, Aqueous environmental Geochemistry, 1997, Prentice Hall Up. Saddle River NJ.
15. S. E. Bone, J. J. Dynes, J. Cliff, J. R. Bargar, Uranium(IV) adsorption by natural organic matter in anoxic sediments, Proc. Natl. Acad. Sci. U. S. A., 2017, 114, 711.
16. G. Dublet, J. Lezama Pacheco, J. R. Bargar, S. Fendorf, N. Kumar, G. V. Lowry, G. E. Brown, Partitioning of uranyl between ferrihydrite and humic substances at acidic and circum-neutral pH, Geochim. Cosmochim. Acta, 2017, Acta 215, 122–140.
17. K.-U. Ulrich, E. S. Ilton, H. Veeramani, J. O. Sharp, R. Bernier-Latmani, E. J. Schofield, J. R. Bargar, D. E. Giammar, Comparative dissolution kinetics of biogenic and chemogenic uraninite under oxidizing conditions in the presence of carbonate. Geochim. Cosmochim. Acta, 2009, 73, 6065–6083.
18. D. E. Latta, K. M. Kemner, B. Mishra, M. I. Boyanov, Effects of calcium and phosphate on uranium(IV) oxidation: Comparison between nanoparticulate uraninite and amorphous UIV–phosphate. Geochim. Cosmochim. Acta, 2016, 174, 122–142.
19. Zhou P., Gu B. Extraction of oxidized and reduced forms of uranium from contaminated soils: effect of carbonate concentration and pH. Environ. Sci and Technol., 2005, 39, 4435-4440.
20. L. Newsome, K. Morris, J. R. Lloyd, The biogeochemistry and bioremediation of uranium and other priority radionuclides, Chem. Geol., 2014, 363, 164–184.
21. D. R. Lovley, E. J. Philips, Y. A., Gorby, E. R., Landa, E. R., Microbial reduction of uranium. Nature, 1991, 350, 413-416.

22. R. Bernier-Latmani, H. Veeramani, E. D. Vecchia, P. Junier, J. S. Lezama-Pacheci, E. I. Suvorova, J. O. Sharp, N. S. Wigginton, J. R. Bargar, Non-uraninite products of microbial U(VI) reduction, Env. Sci. Technol., 2010, 44, 9456-9462.

23. D. R., Brookshaw, R. A. D. Pattrick, P. Bots, G. T. W. Law, J. R. Lloyd, J. F. W. Mosselmans, D. J. Vaughan, K. Dardenne, K. Morris, Redox interactions of Tc(VII), U(VI) and Np (V) with microbially reduced biotite and chlorite, Environ. Sci. Technol., 2015, 49, 13139-13148.

24. E. J. O'Loughlin, S. D. Kelly, R. E. Cook, R. Csencsits, K. M. Kemner, Reduction of uranium(VI) but mixed iron(II)/iron(III) hydroxide (green rust): formation of UO2 nanoparticles., Environ. Sci. Technol., 2003, 37, 721-727.

25. M. Ginder-Vogel, B. Stewart, S. Fendorf, Kinetic and mechanistic constraints on the oxidation of biogenic uraninite by ferrihydrite, Environ. Sci. Technol., 2010, 44, 163-169.

26. J. M. Senko, Y. Mohamed, T. A. Dewers, L. R. Krumholz, Role of Fe(III) minerals in nitrate-dependent microbial U(IV) oxidation, Environ. Sci. Technol., 2005, 39, 2529-2536.

27. M. J. Beazley, R. J. Martinez, P. A. Sobecky, S. M. Webb, M. Taillefert, Nonreductive biomineralization of uranium(VI) phosphate via microbial phosphatase activity in anaerobic conditions, Geomicrob. J., 2009, 26, 431-441.

28. I., Llorens, G. Untereiner, D. Jaillard, B. Gouget, V. Chapon, M. Carriere, Uranium interaction with two multi-resistant environmental bacteria: *cupriavidus metallidurans* CH34 and *rhodopseudomonas palustris*, Plos One, 2012, 7, e51873.

29. M. Kalin, W. N. Wheeler, G. Meinrath, The removal of uranium from mining waste water using algal/microbial biomass, J. Environ. Radioact., 2005, 78, 151–177.

30. M. Seder-Colomina, G. Morin, J. Brest, G. Ona-Nguema, N. Gordien, J.-J. Pernelle, D. Banerjee, O. Mathon, G. Esposito, E. D. van Hullebusch, Uranium(VI) Scavenging by Amorphous Iron Phosphate Encrusting Sphaerotilus natans Filaments, Environ. Sci. Technol., 2015, 49, 14065–14075.

31. F. G. Ferris, R. O. Hallberg, B. Lyvén, K. Pedersen, Retention of strontium, cesium, lead and uranium by bacterial iron oxides from a subterranean environment, Appl. Geochem., 2000, 15, 1035-1042.

32. I. A. Katsoyiannis, Carbonate effects and pH-dependence of uranium sorption onto bacteriogenic iron oxides: kinetic and equilibrium studies. J Hazard. Mater., 2007, 139, 31-37.
33. M. Seder-Colomina, G. Morin, K. Benzerara, G. Ona-Nguema, J.-J. Pernelle, G. Esposito, E. D. van Hullebusch, Sphaerotilus natans, a neutrophilic-iron related sheath-forming bacterium: perspective for metal remediation strategies. Geomicrob. J., 2014, 31, 64-75.
34. M. L. Merroun, S. Selenska-Pobell, Bacterial interactions with uranium: an environmental perspective. J. Contam. Hydrol., 2008, 102, 285-295.
35. U. K. Banala, N. P. I. Das, S. R. Toleti, Microbial interactions with uranium: towards an effective bioremediation approach, Env. Technol. Innov., 2021, 21, 101254.
36. M. Bader, K. Müller, H. Foerstendorf, M. Schmidt, K. Simmons, J. S. Swanson, D. T. Reed, T., Stumpf, A. Cherkouk, Comparative analysis of uranium bioassociation with halophilic bacteria and archaea, Plos One, 2018, 13, e0190953.
37. G. Radeva, A. Kenarova, V. Bachvarova, K. Flemming, I. Popov, D. Vassilev, S. Selenska-Pobell, Phylogenetic diversity of archaea and the archaeal ammonia monooxygenase gene in uranium mining-impacted locations in Bulgaria, Archaea, 2014, 196140.
38. J. A. Siles, R. Margesin, Abundance and Diversity of Bacterial, Archaeal, and Fungal Communities Along an Altitudinal Gradient in Alpine Forest Soils: What Are the Driving Factors? Microb. Ecol., 2016, 72, 207–220.
39. C. Reitschuler, K. Hofmann, P. Illmer, Abundances, diversity and seasonality of (non-extremophilic) Archaea in Alpine freshwaters. Antonie Van Leeuwenhoek, 2016, 109, 855–868.
40. K. M.Campbell, R. K. Kukkadapu, N. P. Qafoku, A. D. Peacock, E. Lesher, K H. Williams, J. R. Bargar, M. J. Wilkins, L. Figueroa, J. Ranville, J. A. Davis, P. E. Long, Geochemical, mineralogical and microbiological characteristics of sediment from a naturally reduced zone in a uranium-contaminated aquifer. Appl. Geochem., 2012, 27, 1499–1511.
41. P. Lefebvre, A. Gourgiotis, A. Mangeret, P. Sabatier, P. Le Pape, O. Diez, P. Louvat, N. Menguy, P. Merrot, C. Baya, M. Zebracki, P. Blanchart, E. Mallet, D. Jézéquel, J.-L. Reyss, J.

R. Bargar, J. Gaillardet, C. Cazala, G. Morin, Diagenetic formation of uranium-silica polymers in lake sediments over 3,300 years, Proc. Nat. Acad. Sci. U. S. A., 2021, 118, 2021844118.

42. D. L. Stoliker, K. M. Campbell, P. M. Fox, D. M. Singer, N. Kaviani, M. Carey, N. Peck, J. R. Bargar, D. B. Kent, J. A. Davis, Evaluating Chemical Extraction Techniques for the Determination of Uranium Oxidation State in Reduced Aquifer Sediments, Environ. Sci. Technol., 2013, 47, 9225–9232.
43. T. L. Bank, R. K. Kukkadapu, A. S. Madden, M. A. Ginder-Vogel, M. E. Baldwin, P. M. Jardine, Effects of gamma-sterilization on the physico-chemical properties of natural sediments, Chem. Geol., 2008, 251, 1-7.
44. G. Sarazin, G. Michard, F. Prevot, A rapid and accurate spectroscopic method for alkalinity measurements in sea water samples, Water Res., 1999, 33, 290–294.
45. E. Viollier, P. Inglett, K. Hunter, A. Roychoudhury, P. Van Cappellen, The ferrozine method revisited: Fe(II)/Fe(III) determination in natural waters. Appl. Geochem., 2000, 15, 785–790.
46. F. Mercier-Bion, R. Drot, J. J. Ehrhardt, J. Lambert, J. Roques, E. Simoni, X-ray photoreduction of U(VI)-bearing compounds, Surf. Interface Anal., 2011, 43, 777–783.
47. B. Ravel, M. Newville, ATHENA, ARTEMIS, HEPHAESTUS: data analysis for X-ray absorption spectroscopy using IFEFFIT, J. Synchro. Rad., 2005, 12, 537–541.
48. G. Morin, F. Juillot, C. Casiot, O. Bruneel, J.-C. Personné, F. Elbaz-Poulichet, M. Leblanc, P. Ildefonse, G. Calas, Bacterial formation of tooeleite and mixed arsenic(III) or arsenic(V)-iron(III) gels in the Carnoulès acid mine drainage, France. A XANES, XRD and SEM study, Env. Sci. Technol., 2003, 37, 1705-1712.
49. M. O. Krause, J. H. Oliver, Natural widths of atomic K and L levels, K α X-ray lines and several KLL Auger lines, J. Phys. Chem. Ref. Data, 1979, 8, 329-338.
50. J. G. Caporaso, C. L. Lauber, W. A. Walters, D. Berg-Lyons, C. A. Lozupone, P. J. Turnbaugh, N Fierer, R. Knight, Global patterns of 16S rRNA diversity at a depth of millions of sequences per sample, Proc. Natl Acad. Sci. U. S. A., 2011,108, 4516−4522.
51. S. Andrews, FastQC: a quality control tool for high throughput sequence data, 2010, http://www.bioinformatics.babraham.ac.uk/projects/fastqc.

52. M. Martin, Cutadapt removes adapter sequences from high-throughput sequencing reads, EMBnet J., 2014 17, 10-12.

53. R. C. Edgar, Search and clustering orders of magnitude faster than BLAST, Bioinformatics, 2010, 26, 2460-2461.

54. J. R. Cole, Q. Wang, J. A. Fish, B. Chai, D. M. McGarrell, Y. Sun, C. T. Brown, A. Porras-Alfaro, C. R. Kuske, J. M. Tiedje, Ribosomal Database Project: data and tools for high throughput rRNA analysis, Nucleic Acids Res., 2014, 42, D633-D642.

55. C. Lozupone, M. Lladser, D. Knights, J. Stombaugh, R. Knight, UniFrac: an effective distance metric for microbial community comparison, ISME J, 2011, 5, 169–172.

56. P. J., McMurdie, S. Holmes, phyloseq: An R Package for Reproducible Interactive Analysis and Graphics of Microbiome Census Data, PLoS One, 2013, 8, e61217.

57. A. Barberán, S. T. Bates, E. O. Casamayor, N. Fierer, Using network analysis to explore co-occurrence patterns in soil microbial communities, ISME J., 2011, 6, 343.

58. G. R. Warnes, B. Bolker, L. Bonebakker, R. Gentleman, W. H. A. Liaw, T. Lumley, M. Maechler, A. Magnusson, S. Moeller, M. Schwartz, gplots: various R programming tools for plotting data. R package version, 2009, 2, 1.

59. D. L. Parkhurst, C. A. J. Appelo, Description and input of examples for PHREEQC Version 3 – A computer program for speciation, batch-reaction, one-dimensional transport, and inverse geochemical calculations, 2016, U.S. Geological Survey Techniques and Methods, book 6, chap. A43, 497 p., available only at http://pubs.usgs.gov/tm/06/a43/.

60. D. Emerson, E. J. Fleming, J. M. McBeth, Iron-oxidizing bacteria: an environmental and genomic perspective, Annu. Rev. Microb., 2010, 64, 561-583

61. S., Hedrich, M. Schlömann, D. B. Johnson, The iron-oxidizing proteobacteria, Microbiology, 2011, 157, 1551–1564.

62. C. Lavire, P. Normand, I. Alekhina, S. Bulat, D. Prieur, J.-L. Birrien, P. Fournier, C. Hänni, J.-R. Petit, Presence of Hydrogenophilus thermoluteolus DNA in accretion ice in the subglacial Lake Vostok, Antarctica, assessed using rrs, cbb and hox, Env, Microb., 2006, 8, 2106-2114.

63. R. J. Birtles, T. J. Rowbotham, R. Michel, D. G. Pitcher, B. Lascola, S. Alexiou-Daniel, D. Raoult, Candidatus Odyssella thessalonicensis' gen. nov., sp. nov., an obligate intracellular parasite of Acanthamoeba species, Int. J. Syst. Evol. Microbiol., 2000, 1, 63-72.

64. N. A. Turner, G. A. Biagini, D. Lloyd, Anaerobiosis-induced differentiation of *Acanthamoeba castellanii*,. FEMS Microb. Lett., 1997, 157, 149-153.

65. I. Sifaoui, E. C. Yanes, M. Reyes-Batlle, R. L. Rodríguez-Expósito, I. L. Bazzocchi, I. A. Jiménez, J. E. Piñero, J. Lorenzo-Morales, L. K. Weaver, 2021, High oxygen concentrations inhibit Acanthamoeba spp, Parasitol. Res., 2021, 120, 3001-3005.

66. K.-U. Ulrich, A. Singh, E. J. Schofield, J. R. Bargar, H. Veeramani, J. O. Sharp, R. Bernier-Latmani, D. E. Giammar, Dissolution of biogenic and synthetic UO_2 under varied reducing conditions, Environ. Sci. Technol., 2008, 42, 5600-5606.

67. G. K., Druschel, D. Emerson, R. Sutka, P. Suchecki, G. W. Luther III, Low-oxygen and chemical kinetic constraints on the geochemical niche of neutrophilic iron(II) oxidizing microorganisms, Geochim. Cosmochim. Acta., 2008, 72, 3358-3370.

68. S. Vollrath, T. Behrens, P. van Cappelen,. Oxygen dependency of neutrophilic Fe(II) oxidation by *Leptothrix* differs from abiotic reaction, Geomicrob. J., 2012, 29, 550-560.

69. R. M. Cornell, U. Schwertmann,. The iron oxides: structure, properties, reactions, occurences and uses, 2003, John Wiley & Sons.

70. C. Hohmann G. Morin, G. Ona-Nguema J. M. Guigner, G. E., Brown Jr, A. Kappler, Molecular-level modes of As binding to Fe(III) (oxyhydr)oxides precipitated by the anaerobic nitrate-reducing Fe(II)-oxidizing Acidovorax sp. strain BoFeN1, Geochimica et Cosmochimica Acta, 2011, 75, 4699-4712.

71. A. Voegelin, R. Kaegi, J. Frommer, D. Vantelon, S. J. Hug, Effect of phosphate, silicate and Ca on Fe(III) precipitates formed in aerated Fe(II)- and As(III)-containing water studied by X-ray absorption spectroscopy, Geochim. Cosmochim. Acta., 2010, 74, 164-186.

72. A.-C. Senn, .R. Kaegi, S. J. Hug, K. G. Hering, S. Mangold, A. Voegelin, Compositon and structure of Fe(III)-precipitates formed by Fe(II) oxidation in water at near-neutral pH:

interdependent effects of phosphate, silicate and Ca, Geochim. Cosmochim. Acta, 2015, 162, 220-246.

73. L. Zhong, C. Liu, J. M. Zachara, D. W. Kennedy, J. E. Szecsody, B. Wood, Oxidative remobilization of biogenic uranium(IV) precipitates: effects on iron(II) and pH, J. Environ. Qual., 2005, 34, 1763-1771.
74. E. Liger, L. Charlet, P. van Cappellen, Surface catalysis of uranium(VI) reduction by iron(II), Geochim. Cosmochim. Acta, 1999, 63, 2939-2955.
75. D. D. Boland, R. N. Collins, T. E. Payne, T. D. Waite, Effect of amorphous Fe(III) oxide transformation on the Fe(II)-mediated reduction of U(VI). Env. Sci. Technol., 2011 45, 1327-1333.
76. E. Krawczyk-Barsch, A. C. Scheinost, A. Rossberg, K. Muller, F. Bok, L. Hallbeck, J. Lehrich, K. Schmeide Uranium and neptunium retention mechanisms in Gallionella ferruginea/ferrihydrite systems for remediation purposes, Env. Sci. Pollut. Res., 2020, 28, 18342-18353.
77. I. S. Kulichevskaya, N. E. Suzina, W. I. C. Rijpstra, J. S. S. Damsté, S. N. Dedysh, Paludibaculum fermentans gen. nov., sp. nov., a facultative anaerobe capable of dissimilatory iron reduction from subdivision 3 of the Acidobacteria. Int. J. Syst. Evol. Microbiol., 2014, 64, 2857–2864.
78. J. Pablo Cárdenas, R. Ortiz, P. R., Norris, E. Watkin, D. S. Holmes, Reclassification of 'Thiobacillus prosperus' Huber and Stetter 1989 as Acidihalobacter prosperus gen. nov., sp. nov., a member of the family Ectothiorhodospiraceae, Int. J. Syst. Evol. Microbiol, 2015, 65, 3641–3644.
79. Lueder U., Jørgensen B. B., Kappler A., Schmidt C. (2020) Fe(III) photoreduction producing Fe_{aq}^{2+} in oxic freshwater sediment. Environ. Sci. Technol., 2020, 54, 862-869.
80. H. Beller, P. Zhou, T. Legler, A. Chakicherla, S. Kane, T. Letain, P. O'Day, Genome-enabled studies of anaerobic, nitrate-dependent iron oxidation in the chemolithoautotrophic bacterium Thiobacillus denitrificans, Front. Microbiol., 2013, 4, 249.

81. J. Schaller, A. Weiske, E. G. Dudel, Effects of gamma-sterilization on DOC, uranium and arsenic remobilization from organic and microbial rich stream sediment, Chem. Geol., 2011, 409, 3211-3214.

82. Lee, JU (Lee, JU) ; Kim, SM (Kim, SM) ; Kim, KW (Kim, KW) ; Kim, IS (Kim, IS) Microbial removal of uranium in uranium-bearing black shale. Chemosphere, 2005, 59, 147-154.